Journal of Fluids and Structures (2001) **15,** 1153–1166
doi:10.1006/jfls.2001.0393, available online at http://www.idealibrary.com on IDEAL®

DYNAMICS AND STABILITY OF PINNED–CLAMPED AND CLAMPED–PINNED CYLINDRICAL SHELLS CONVEYING FLUID†

A. K. Misra, S. S. T. Wong and M. P. Païdoussis

Department of Mechanical Engineering, McGill University
Montreal, Qué., Canada H3A 2K6

(Received 10 August 2000, and in final form 29 January 2001)

The paper examines the dynamics and stability of fluid-conveying cylindrical shells having pinned–clamped or clamped–pinned boundary conditions, where "pinned" is an abbreviation for "simply supported". Flügge's equations are used to describe the shell motion, while the fluid-dynamic perturbation pressure is obtained utilizing the linearized potential flow theory. The solution is obtained using two methods — the travelling wave method and the Fourier-transform approach. The results obtained by both methods suggest that the negative damping of the clamped–pinned systems and positive damping of the pinned–clamped systems, observed by previous investigators for any arbitrarily small flow velocity, are simply numerical artefacts; this is reinforced by energy considerations, in which the work done by the fluid on the shell is shown to be zero. Hence, it is concluded that both systems are conservative.

1. INTRODUCTION

Thin tubes conveying fluid exhibit shell-type vibrations, i.e., their motion not only consists of lateral displacements, but can also involve deformation of the cross-section, the so-called "breathing" modes. This behaviour was discovered by Païdoussis & Denise in 1969, while experimenting with thin, short, cantilevered tubes conveying low-pressure air (Païdoussis & Denise 1971). Subsequent experiments showed that the new shell-type instability observed for cantilevered tubes (shells) can also occur for clamped–clamped ones. The dynamics and stability of these shells were also studied theoretically by Païdoussis & Denise (1972) using Flügge's equations and linearized potential flow theory. The results obtained matched with the experimental ones that cantilevered shells lose stability by flutter at sufficiently high flow velocities; in the case of clamped–clamped shells, which represent a conservative gyroscopic system according to the theoretical model, stability is lost by divergence, followed by coupled-mode flutter at a slightly higher flow velocity. The theoretical study of clamped–clamped shells by Weaver & Myklatun (1973) also produced similar results. The case of simply supported shells was investigated theoretically by Weaver & Unny (1973) and Shayo & Ellen (1974) with the aid of the Flügge-Kempner shell equation, and by Matsuzaki & Fung (1977) utilizing Morley's shell equation. In all cases, linearized potential flow theory was used.

The conclusion from these studies is as follows: if the shell is either clamped or pinned at *both* ends, it is a conservative system and the frequencies remain real (i.e., there is no

† A partial, abridged account of this work was given at the *Canadian Congress of Applied Mechanics*, Memorial University, St. John's, Newfoundland, Canada, in June 2001 (*Proceedings, CANCAM 2001*, Vol. 1, pp. 35–36).

damping), until a certain critical flow velocity is reached where the system loses stability by divergence when the lowest frequency becomes purely imaginary. This is followed by coupled-mode flutter at a slightly higher flow velocity.

In all the studies discussed so far, shells with supported ends had the *same* support condition at both ends: either clamped or simply supported. The dynamics in cases of mixed support conditions, i.e., shells clamped at one end and simply supported at the other ("clamped–pinned" and "pinned–clamped" in short, the first word in each case referring to the upstream end and the second to the downstream one) were studied for the first time by Horáček & Zolotarev (1984) and Zolotarev (1987).

In the first of these two papers, Vol'mir's semi-membrane shell theory was used, which is similar to Donnell's and Morley's, involving only one equation in which most of the higher derivatives with respect to the axial coordinate are absent. In Zolotarev (1987), the Goldenveizer–Novozhilov equations are used, which are similar to Flügge's, but differ in some details; the ends are supported by translational and rotational springs so that, by setting the values of appropriate spring constants to zero or infinity, various simple boundary conditions (clamped, pinned, free, etc.) can be obtained. The perturbation pressure was expressed in travelling-wave form and the method of solution was similar to that of Païdoussis & Denise (1972).

Calculations by Zolotarev with clamped–clamped, pinned–pinned and cantilevered shells showed qualitatively similar behaviour to that obtained in the previous studies. However, clamped–pinned and pinned–clamped shells, which had not been studied earlier, displayed unusual behaviour. Both pinned–clamped and clamped–pinned shells were found to behave as nonconservative systems, although they are conventionally considered as conservative. For a pinned–clamped system, the imaginary part of the complex frequency was found to be positive, implying flow-induced damping, for all values of flow velocity starting from zero, to the critical value when the shell loses stability by divergence. On the other hand, calculations by Païdoussis *et al.* (1993) using Flügge's equations in conjunction with the standing-wave Fourier-transform theory have shown that pinned–clamped shells conveying fluid have a purely real frequency (i.e., no damping) for any flow velocity lower than the critical velocity (for divergence). The question then arises as to which one of these two theories describes the dynamics correctly.

An even more perplexing feature in Horáček and Zolotarev's calculations is the fact that, for clamped–pinned shells, the imaginary part of the complex frequency is negative, implying negative damping, i.e., *instability*, for any flow velocity greater than zero! This is, of course, consistent with Horáček and Zolotarev's results for pinned–clamped shells described earlier. A clamped–pinned system may be considered to be a pinned–clamped one with the flow direction reversed. A change in the sign of the flow velocity causes a change in the sign of the imaginary part of the complex frequency; thus, a positive damping for pinned–clamped systems implies a negative damping for clamped–pinned ones. However, this is at variance with calculations by Païdoussis *et al.* (1993), who have found the clamped–pinned system to be stable, until stability is lost by divergence.

The goal of the present paper is to resolve this apparent paradoxical behaviour of pinned–clamped and clamped–pinned systems.

2. THEORETICAL MODEL

A careful examination of the dynamics of shell systems with mixed boundary conditions is carried out using two different theories: the standing-wave Fourier-transform theory developed by Païdoussis *et al.* (1984) and the travelling wave theory presented by Païdoussis & Denise (1972). In both theories, Flügge's equations are used to describe the motion of the

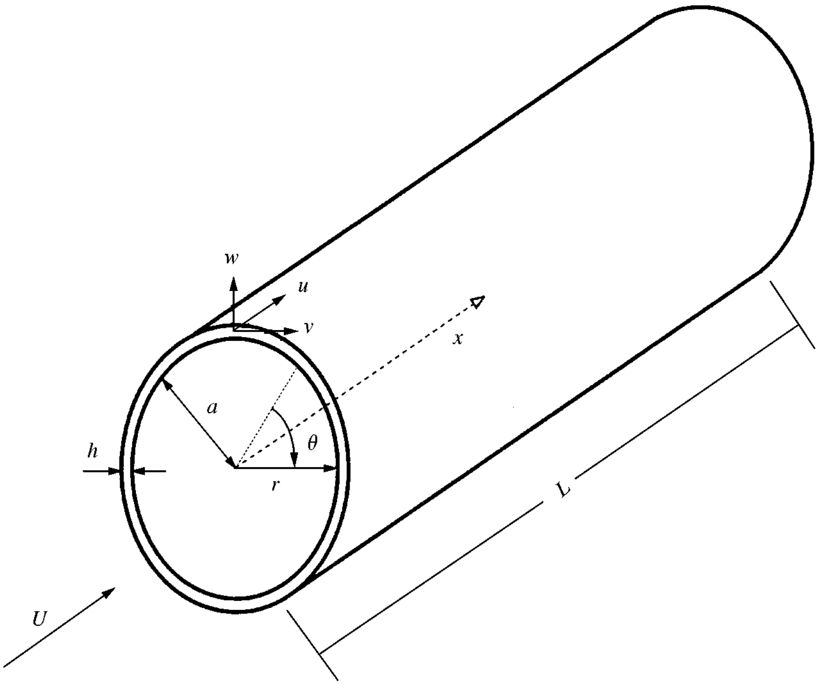

Figure 1. The shell under consideration with some parameters defined.

shell and potential flow theory is used for fluid motions. The two theories are described briefly here; for details the reader is referred to the two works cited in the foregoing or to Païdoussis (2001).

A uniform cylindrical shell of length L, mean radius a and thickness h is considered (Figure 1). The shell material is characterized by the density ρ_s, Young's modulus E and Poisson's ratio ν. In terms of the displacements of the middle surface of the shell, $u(x,\theta,t)$, $v(x,\theta,t)$ and $w(x,\theta,t)$, in the axial, circumferential and radial directions, respectively, the equations of motion are

$$u'' + \frac{1-\nu}{2}u^{\cdot\cdot} + \frac{1+\nu}{2}v'^{\cdot} + \nu w' + k\left[\frac{1-\nu}{2}u^{\cdot\cdot} - w''' + \frac{1-\nu}{2}w'^{\cdot\cdot}\right] = \gamma\frac{\partial^2 u}{\partial t^2},$$

$$\frac{1+\nu}{2}u'^{\cdot} + v^{\cdot\cdot} + \frac{1-\nu}{2}v'' + w^{\cdot} + k\left[\frac{3}{2}(1-\nu)v'' - \frac{3-\nu}{2}w''^{\cdot}\right] = \gamma\frac{\partial^2 v}{\partial t^2}, \tag{1}$$

$$\nu u' + v^{\cdot} + w + k\left[\frac{1-\nu}{2}u'^{\cdot\cdot} - u''' - \frac{3-\nu}{2}v''^{\cdot} + \nabla^4 w + 2w^{\cdot\cdot} + w\right] = -\gamma\left[\frac{\partial^2 w}{\partial t^2} - \frac{q}{\rho_s h}\right],$$

where $(\ )'$ and $(\ )^{\cdot}$ stand for $a\partial(\ )/\partial x$ and $\partial(\ )/\partial\theta$, respectively, q is the radial fluid dynamic loading per unit area of the middle surface, equal to the internal pressure, $k = h^2/12a^2$, $\gamma = \rho_s a^2(1-\nu^2)/E$ and $\nabla^2 = a^2\partial^2/\partial x^2 + \partial^2/\partial\theta^2$.

If the shell is clamped at one of its edges, there is neither displacement nor rotation, so that

$$u = v = w = 0, \qquad \frac{\partial w}{\partial x} = 0. \tag{2}$$

On the other hand, if the end is simply supported, then

$$\begin{aligned} &v = w = 0, \\ &M_x = 0 \qquad\qquad \rightarrow w'' + \nu w^{\cdot\cdot} - \nu v^{\cdot} - u' = 0, \\ &u = 0 \ \text{ or } \ N_x = 0 \rightarrow u' + \nu v^{\cdot} + \nu w - k w'' = 0. \end{aligned} \tag{3}$$

The last boundary condition needs some explanation. A simply supported end may or may not be restrained to move axially. If axial motion is not allowed, $u = 0$; otherwise the axial force $N_x = 0$.

Consider now the interaction of the shell with the fluid. It is assumed that the flow is inviscid and irrotational. Hence, there exists a scalar potential function $\Psi(x, \theta, r, t)$, from which the velocity may be obtained through

$$\mathbf{V} = \nabla \Psi. \tag{4}$$

The potential Ψ consists of two components: one due to the mean flow associated with the undisturbed flow velocity U in the x-direction, and the unsteady component $\Phi(x, \theta, r, t)$ describing the perturbations caused by the shell motions. Hence,

$$\Psi = Ux + \Phi, \tag{5}$$

so that the velocity components of the perturbed flow field are given by

$$V_x = U + \partial\Phi/\partial x, \qquad V_\theta = (1/r)\,\partial\Phi/\partial\theta, \qquad V_r = \partial\Phi/\partial r. \tag{6}$$

The unsteady pressure P is related to the velocity potential Φ by Bernoulli's equation for unsteady flow,

$$\partial\Phi/\partial t + \tfrac{1}{2}V^2 + P/\rho = P_s/\rho, \tag{7}$$

where $V^2 = V_x^2 + V_y^2 + V_z^2$, P_s is the stagnation pressure and ρ is the density of the fluid flowing in the shell. Assuming small disturbances, one can obtain from equation (7)

$$p = -\,\rho(\partial\Phi/\partial t + U\,\partial\Phi/\partial x), \tag{8}$$

where p, the difference between P and $P_s - \frac{1}{2}\rho U^2$, is the perturbation pressure. Hence, the perturbation pressure field can be determined if the potential Φ is known.

The governing equation for potential flow is

$$\nabla^2 \Psi = 0. \tag{9}$$

Substitution of equation (5) into equation (9) yields

$$\nabla^2 \Phi = 0, \tag{10}$$

which must be solved using the boundary condition provided by the impermeability of the surface of the shell, expressed mathematically as

$$V_r = \partial\Phi/\partial r|_{r=a} = (\partial w/\partial t + U\,\partial w/\partial x). \tag{11}$$

Since the boundary condition for Φ involves the radial displacement w of the shell, equations (1) and (10) must be solved simultaneously using boundary conditions (2), (3) and (11), and the loading given by equation (8).

3. METHODS OF SOLUTION

As mentioned earlier, two methods of solution are used: the travelling-wave method presented by Païdoussis & Denise (1972) and the standing-wave Fourier-transform approach by Païdoussis *et al.* (1984). They are described below briefly.

3.1. Travelling-Wave Method

In this method, a solution is sought in the form of waves travelling along the shell, i.e., the shell displacements have the form

$$\begin{aligned} u &= A\exp[\mathrm{i}(\lambda x/a + n\theta + \omega t)], \\ v &= B\exp[\mathrm{i}(\lambda x/a + n\theta + \omega t)], \\ w &= C\exp[\mathrm{i}(\lambda x/a + n\theta + \omega t)], \end{aligned} \tag{12}$$

where A, B, C are complex coefficients, and n is the circumferential wavenumber. Similarly, the potential Φ may be expressed as

$$\Phi = R(r)\exp[\mathrm{i}(\lambda x/a + n\theta + \omega t)], \tag{13}$$

where $R(r)$ is a function to be determined. Substitution of equation (13) into equation (10), use of boundary condition (11) and the fact that $R(r)$ must be finite everywhere, yield the solution for Φ in terms of modified Bessel functions. Application of equation (8) then yields the perturbation internal pressure as (Païdoussis & Denise 1972)

$$p = -\rho\frac{a}{n + \lambda I_{n+1}(\lambda)/I_n(\lambda)}\left(\frac{\partial}{\partial t} + U\frac{\partial}{\partial x}\right)^2 w, \tag{14}$$

where $I_n(\lambda)$ is the modified Bessel function of first kind and of order n. Substitution of equations (14) and (12) into equation (1) leads to three linear homogeneous equations in the unknowns A, B, C. For nontrivial solution, the associated determinant must vanish. This results in a transcendental equation in λ (because of the modified Bessel functions in the pressure expression); hence, this characteristic equation has an infinite number of roots, implying that the total solution for u, v and w should be written as

$$\begin{aligned} u &= \sum_{j=1}^{\infty} A_j\exp[\mathrm{i}(\lambda_j x/a + n\theta + \omega t)], \\ v &= \sum_{j=1}^{\infty} B_j\exp[\mathrm{i}(\lambda_j x/a + n\theta + \omega t)], \\ w &= \sum_{j=1}^{\infty} C_j\exp[\mathrm{i}(\lambda_j x/a + n\theta + \omega t)]. \end{aligned} \tag{15}$$

However, the total number of boundary conditions at the two ends of the shell, represented by equations (2) and (3), is eight; hence, a truncated set of eight λ's are retained in equation (15). Substitution of equation (15) into the boundary conditions (2) and (3) yields a set of homogeneous linear algebraic equations in A_j, B_j and C_j; again, for nontrivial solution of these equations, the determinant of their coefficients must vanish, which yields the frequency equation. Starting from some initial value for the frequency, we iterate to find the values of the (complex) frequency that satisfy this frequency equation.

3.2. Standing Wave Solution

In this approach, the solution is expressed in the form

$$\begin{aligned} u &= \sum_{m=1}^{\infty} A_{mn}\cos n\theta\, a[\mathrm{d}\phi_m(x)/\mathrm{d}x]\exp(\mathrm{i}\omega t), \\ v &= \sum_{m=1}^{\infty} B_{mn}\sin n\theta\, \phi_m(x)\exp(\mathrm{i}\omega t), \\ w &= \sum_{m=1}^{\infty} C_{mn}\cos n\theta\, \phi_m(x)\exp(\mathrm{i}\omega t), \end{aligned} \tag{16}$$

where m and n are axial and circumferential wavenumber, respectively, while $\phi_m(x)$ are the eigenfunctions of a uniform beam having the same support conditions as the shell. Due to the orthogonality of the sin $n\theta$ and cos $n\theta$ functions, circumferential modes are decoupled and hence there is no summation over n in equation (16).

The perturbation velocity potential is assumed to have the form

$$\Phi(x, r, \theta, t) = \Psi_n(x, r) \cos n\theta \exp(\mathrm{i}\omega t), \tag{17}$$

where Ψ_n is an unknown function associated with circumferential mode n and is to be determined. Substituting equation (17) into equation (10) and taking its Fourier transform, one obtains an ordinary differential equation whose solution can be written in terms of the modified Bessel functions of order n. Using boundary condition (11) and pressure expression (8), and taking the inverse Fourier transform, the expression for the radial load q can be determined as

$$q = \sum_{m=1}^{\infty} Q_{mn}(\xi) \cos n\theta \exp(\mathrm{i}\omega t), \tag{18}$$

where

$$Q_{mn}(\xi) = (\rho U^2 C_{mn}/2\pi L^2) \int_{-\infty}^{\infty} \frac{(\kappa_i - \bar{\alpha})^2}{\mu L} E_n(\bar{\alpha}, a)\, \phi_m^*(\bar{\alpha})\, \mathrm{e}^{-\mathrm{i}\bar{\alpha}\xi}\, \mathrm{d}\bar{\alpha} \tag{19}$$

and

$$\xi = x/L, \qquad \kappa_i = \omega L/U, \qquad \bar{\alpha} = \alpha L, \qquad E_n(\bar{\alpha}, r) = I_n(\bar{\alpha} r)/I_n'(\bar{\alpha} a). \tag{20}$$

In the foregoing, α is the Fourier-transform variable, the asterisk denotes a transformed quantity, I_n is the modified Bessel function of the first kind of order n, and $I_n'(z) = \mathrm{d}\, I_n(z)/\mathrm{d}z$.

Equations (16) and (18) can now be substituted into equations of motion (1) and integrated over the length to yield a standard eigenvalue problem. Solution of this eigenvalue problem yields the complex frequencies.

4. RESULTS

To test the validity of the computer programs first, calculations were carried out for the clamped–clamped (C–C) configuration with the same parameters as those used by Païdoussis & Denise (1972) for a rubber–air system (i.e., a rubber shell conveying air) and by Païdoussis *et al.* (1984) for a steel–water system. These parameters are shown in Table 1. The results are presented in nondimensional form using the following quantities:

$$\bar{\omega} = [E/\{\rho_s(1 - \nu^2)\, a^2\}]^{-1/2}\omega, \qquad \bar{U} = [E/\{\rho_s(1 - \nu^2)\}]^{-1/2} U. \tag{21}$$

Figure 2 shows the variation of $\mathscr{Re}(\bar{\omega})$ and $\mathscr{Im}(\bar{\omega})$ with $\bar{U}$ for the C–C rubber–air system.† It may be noted that the imaginary part of $\bar{\omega}$ is zero until the system loses stability by divergence at the nondimensional speed of $\bar{U} = 0{\cdot}580$, which matches with the results of Païdoussis & Denise (1972) to three significant figures. Subsequently, the second mode becomes unstable by divergence at 0·606, followed immediately by coupled-mode flutter at 0·610.

The results for the C–C steel–water system are shown in Figure 3. These are almost identical (to within 1·5%) to those obtained by Païdoussis *et al.* (1984). Again, the imaginary

† The parameters in Table 1 define the systems considered completely. For brevity, we refer to them often as "the rubber–air system", and so on.

TABLE 1
Shell and fluid parameters used in the calculations

System	h (mm)	a (mm)	L (m)	ρ_s (kg/m^3)	E (N/m^2)	ν (—)	ρ (kg/m^3)
Rubber–air	0·178	7·9	0·204	895	$3{\cdot}4 \times 10^5$	0·47	1·21
Steel–water	0·5	90	1·0	7715	$1{\cdot}06 \times 10^{11}$	0·30	998·6
Zolotarev	0·2	150	1·0	2800	$7{\cdot}2 \times 10^{10}$	0·34	12·0

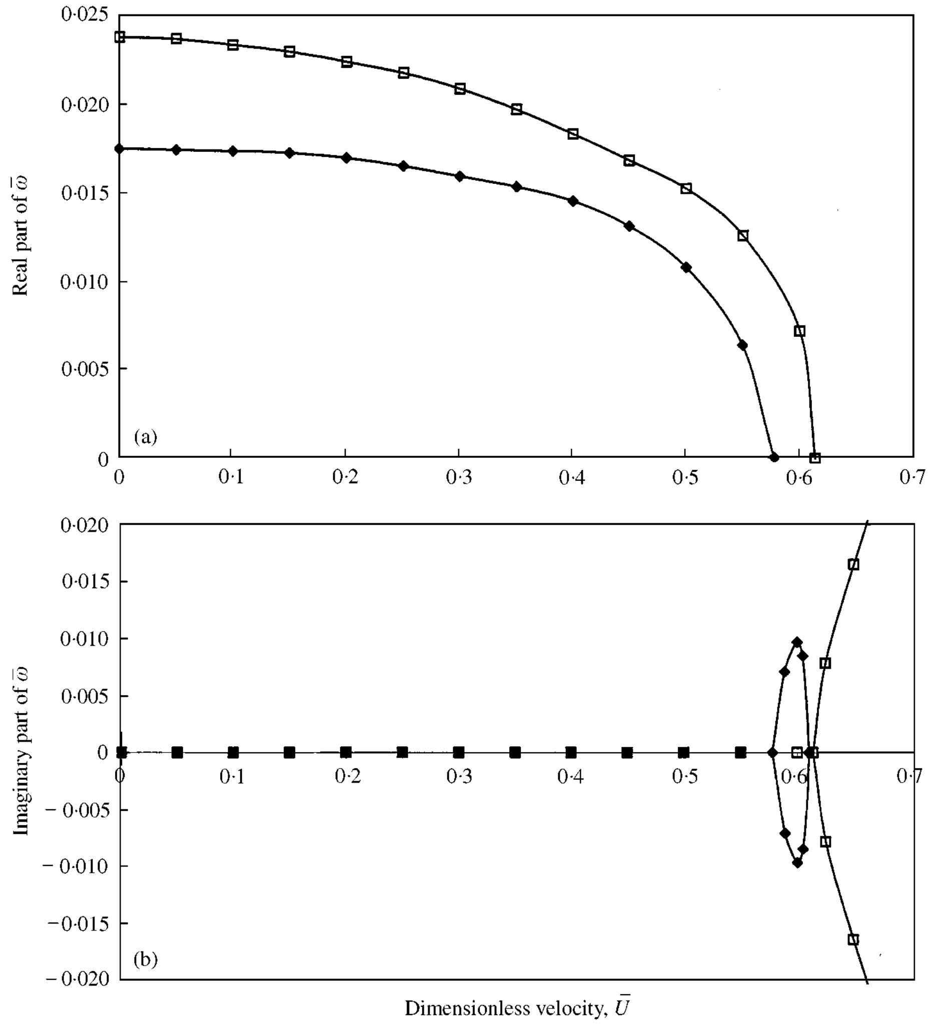

Figure 2. (a) The real and (b) the imaginary components of the dimensionless complex frequency, $\bar{\omega}$, as functions of the dimensionless flow velocity $\bar{U}$, for a clamped–clamped rubber shell conveying air (the "rubber–air system"), as obtained by the travelling wave analysis for, $n = 2$, and other parameters as in Table 1. ◆, $m = 1$; □, $m = 2$.

part of the frequency is zero, until the system loses stability by divergence at $\bar{U} = 0{\cdot}026$, identical to that reported by Païdoussis *et al.* Then, the system is restabilized briefly, before the onset of coupled-mode flutter, again as in Païdoussis *et al.* Hence, the computer codes developed seem to be reliable.

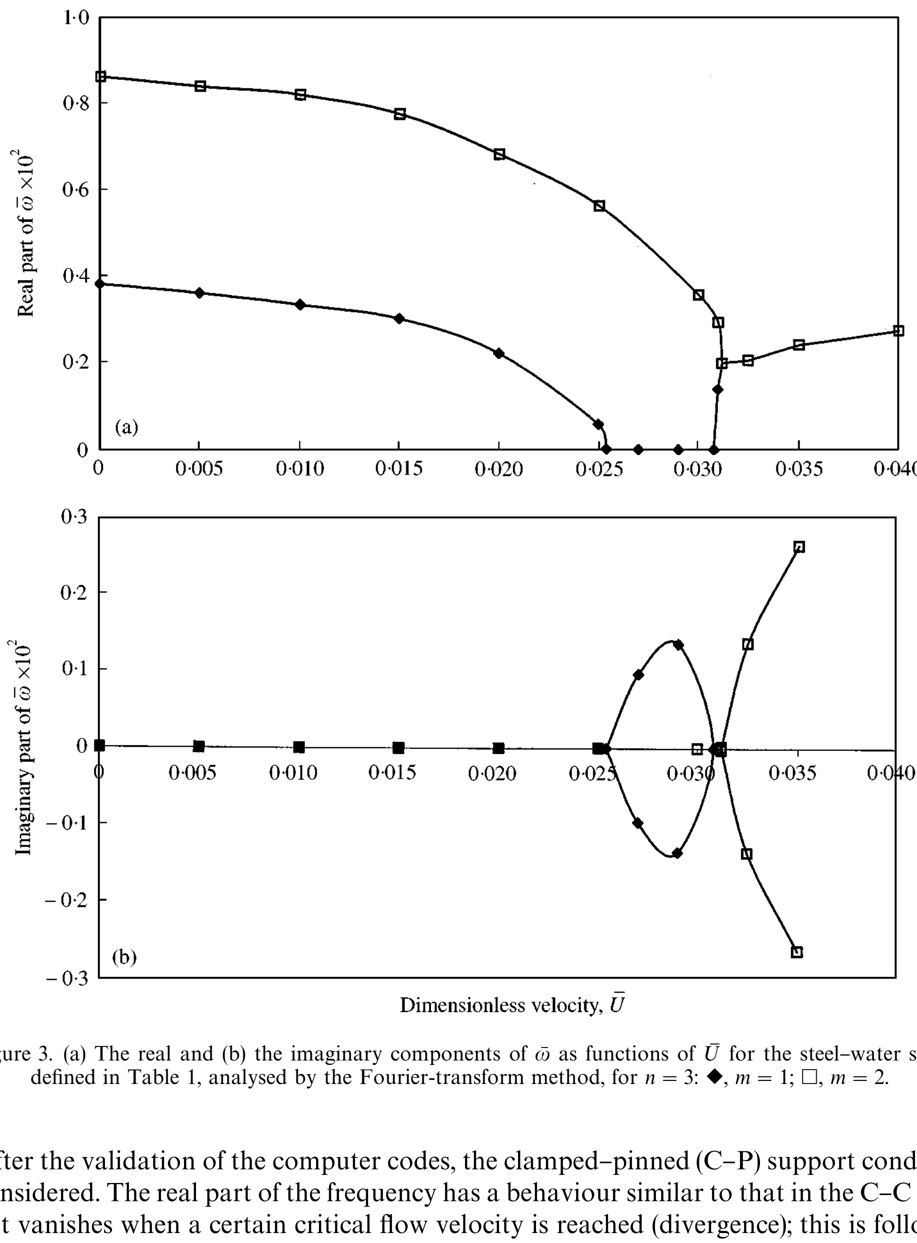

Figure 3. (a) The real and (b) the imaginary components of $\bar{\omega}$ as functions of $\bar{U}$ for the steel–water system defined in Table 1, analysed by the Fourier-transform method, for $n = 3$: ◆, $m = 1$; □, $m = 2$.

After the validation of the computer codes, the clamped–pinned (C–P) support condition is considered. The real part of the frequency has a behaviour similar to that in the C–C case, i.e., it vanishes when a certain critical flow velocity is reached (divergence); this is followed by a combination of the first two modes, corresponding to coupled-mode flutter. However, the imaginary parts display an interesting and unusual behaviour. Figure 4 shows the results obtained using the Fourier-transform method for the C–P support condition of the three shell systems described in Table 1. $\mathscr{I}m(\bar{\omega})$ has been plotted using a highly expanded scale; otherwise it will appear to be almost zero. It may be noticed that $\mathscr{I}m(\bar{\omega})$ is negative, i.e., these shell systems appear to have negative damping and are therefore unstable for any flow velocity greater than zero! The magnitude of this negative damping increases with the flow velocity, almost linearly in the case of the rubber–air system. Similar results are also obtained if the travelling-wave method is used with $u = 0$ or $N_x = 0$.

On the other hand, if the boundary conditions are changed to P–C, the damping becomes positive for any arbitrarily small flow velocity, as shown for the steel–water system in

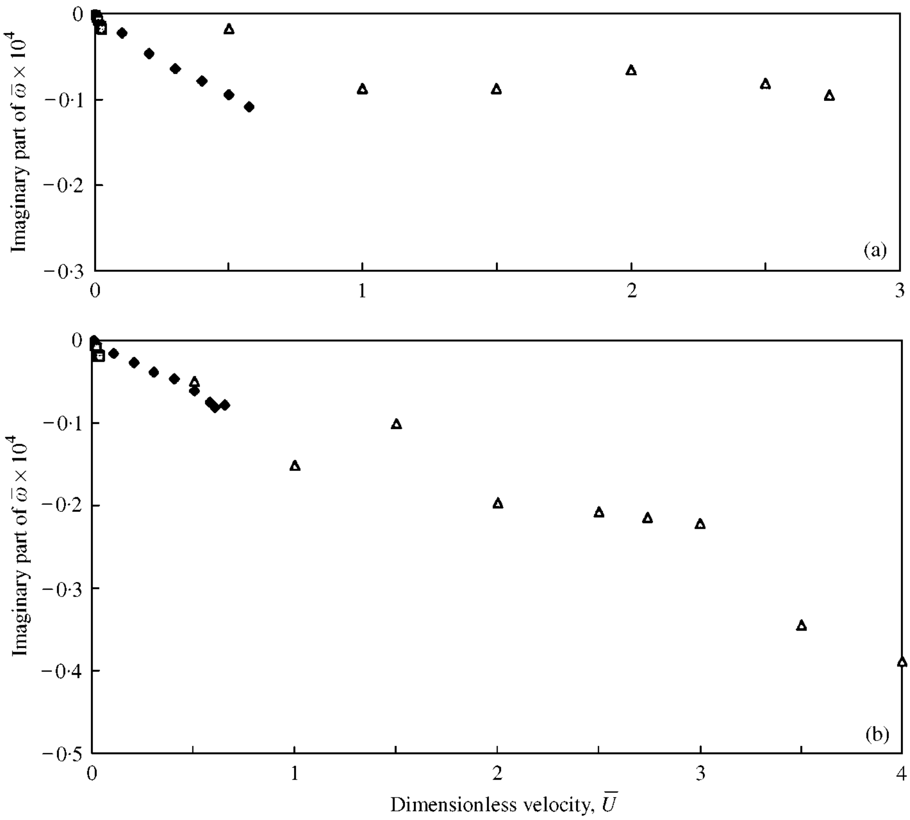

Figure 4. The imaginary components of the complex frequency $\bar{\omega}$, for different *clamped–pinned* shell–fluid systems, analysed by the Fourier-transform method: △, Zolotarev's system ($n = 2$); ♦, Païdoussis & Denise's rubber–air system ($n = 2$); □, the Païdoussis *et al.* steel–water system ($n = 2$). (a) For the first mode, $m = 1$; (b) for the second mode, $m = 2$.

Figure 5(b). The value of the positive damping for a given flow velocity is equal to that of the negative damping for the C–P case, as seen in Figure 5(a). These results are similar to those presented in Zolotarev (1987). The imaginary parts are approximately three orders of magnitude smaller than the real parts; among the three systems considered, the third system, corresponding to the Zolotarev parameters, yields the largest $\mathscr{I}m(\omega)$, in rad/s.

The question arises as to whether these results represent a true physical phenomenon or are simply a numerical artefact. In order to resolve this, an investigation of the possible sources of numerical inaccuracy was carried out for the two methods—the Fourier-transform approach and the travelling-wave method. In both methods, numerical error can be reduced by using long double (quadruple) precision arithmetic. However, the major source of inaccuracy in the Fourier-transform method is the approximate nature of the eigenvalues used to calculate the beam eigenfunctions $\phi_m(x)$ appearing in equation (16). These eigenvalues are the solution to a transcendental characteristic equation corresponding to the support conditions of the shell and must be evaluated numerically. Accuracy of this evaluation has a significant effect on that of the solution of the overall problem, as shown below. On the other hand, the accuracy of the travelling-wave solution depends strongly on the tolerance imposed on the determination of the λ's (nondimensional wavenumbers) appearing in equation (12).

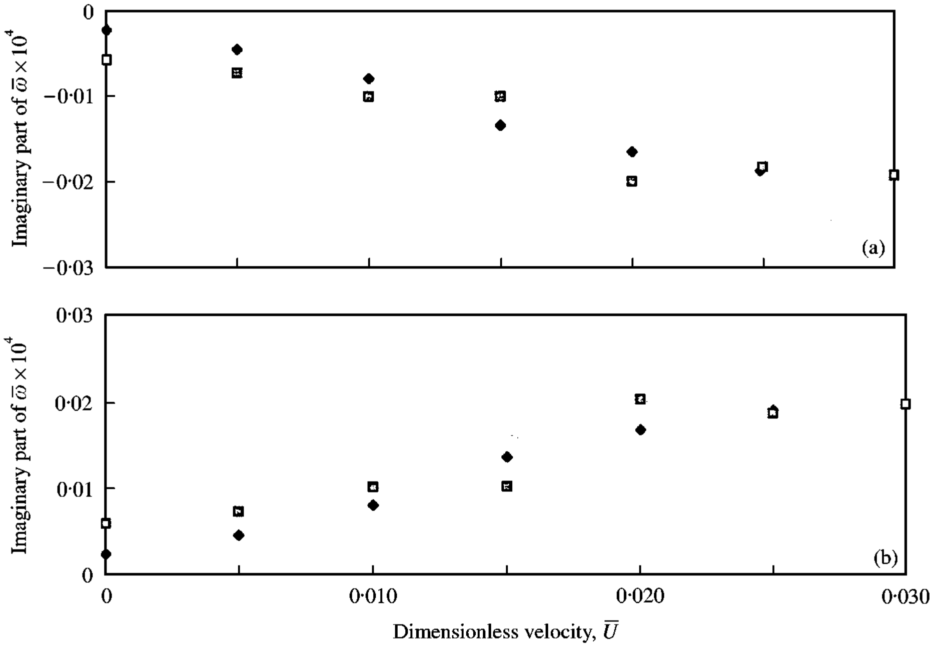

Figure 5. The imaginary component of $\bar{\omega}$ versus $\bar{U}$ for the steel–water system, analysed by the Fourier-transform method: (a) clamped–pinned; (b) pinned–clamped. ◆, $m = 1$; □, $m = 2$.

Figure 6 shows the variation of $\mathscr{I}m(\bar{\omega})$ with the number of significant digits to which the beam eigenvalues have been calculated accurately; these results were obtained using the Fourier-transform technique for the C–P rubber–water system for $\bar{U} = 0{\cdot}3$, Figure 6(a), and 0·4, Figure 6(b). The value of $-\mathscr{I}m(\bar{\omega})$, negative damping, is small (of the order of 10^{-5}). It is greater for the axial mode $m = 2$ compared to $m = 1$, and is larger for higher flow velocity. However, it is clear that for both axial modes, the negative damping decreases monotonically when the number of accurate significant figures in the beam eigenvalues increases from 8 to 18. It appears that, in the limit, the negative damping should reach zero, implying a conservative undamped behaviour of the system. Hence, the occurrence of "instability" of the C–P system for any small nonzero flow velocity appears to be a numerical artefact and is not likely to be realized in practice.†

The accuracy of the travelling-wave solution is examined next. The same C–P rubber–air system is considered again. The changes in $\mathscr{I}m(\bar{\omega})$, when the tolerance in the solution of the λ's is tightened, are shown in Figure 7 for various values of the nondimensional velocity $\bar{U}$. It is clear that $\mathscr{I}m(\bar{\omega})$ tends to zero for both $m = 1$ and 2 when the tolerance is made smaller. Hence, both solution methods lead to the conclusion that, for ideal calculations, the clamped–pinned system is a conservative one involving zero damping until the system loses stability by divergence for a sufficiently high flow velocity.

As opposed to the clamped-pinned system, the pinned-clamlped system is better behaved numerically; in calculations with the standing wave solution the imaginary part of the frequency is found to be at least 30% closer to zero. This might be related to the form of the

† Thus, the conclusion reached earlier by Païdoussis *et al.* (1993) is upheld, although in that paper no exhaustive study was undertaken of how close $\mathscr{I}m(\bar{\omega})$ really is to zero.

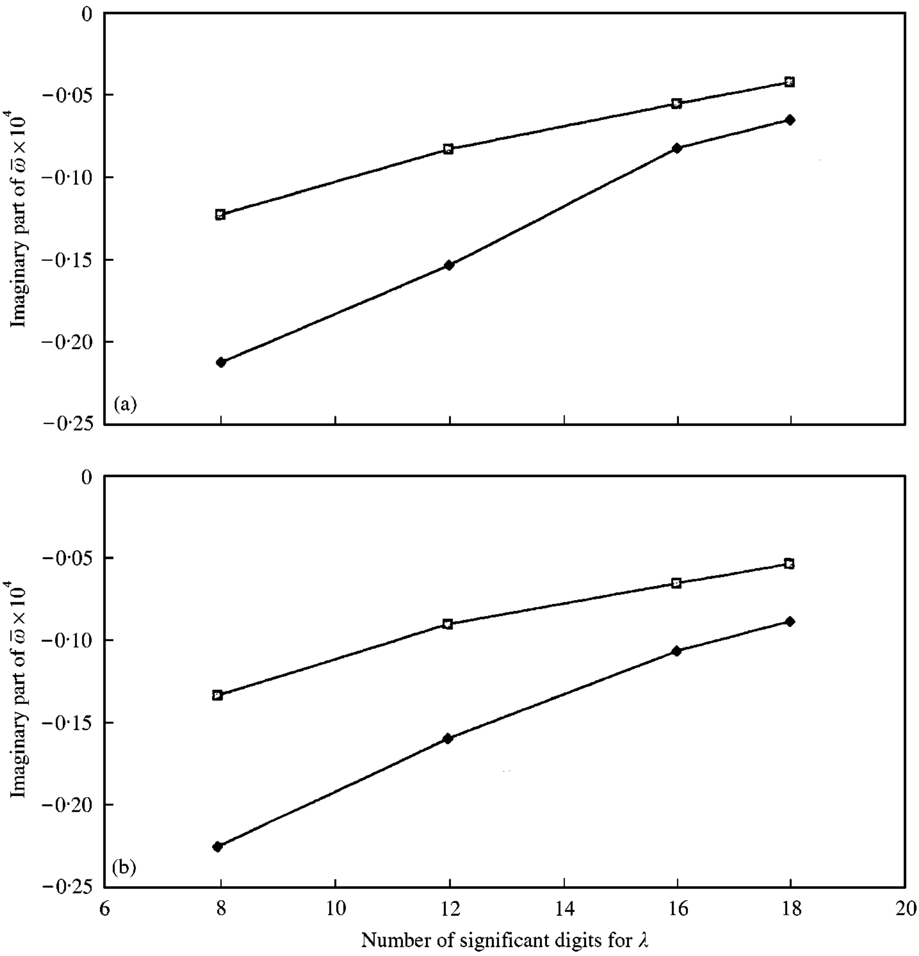

Figure 6. The effect of the number of significant digits utilized for the determination of the λ's on the computed imaginary component of $\bar{\omega}$ for the clamped-pinned rubber–air system ($n = 2$), analysed by the Fourier-transform method: (a) for $\bar{U} = 0{\cdot}3$; (b) for $\bar{U} = 0{\cdot}4$. ♦, $m = 1$; □, $m = 2$.

eigenfunctions that makes the numerics very sensitive to precision in one case but not the other.‡

Some further calculations were conducted by the travelling wave method for a pinned-clamped (P-C) system with reverse flow (with flow velocity $-U$ instead of U)—thus *physically* for the C-P system considered before in Figure 7. However, the results show that this P-C system is much less sensitive to imprecision: for the tightest tolerances of Figure 7, in this case $\mathscr{I}m(\bar{\omega}) = 0 \pm 10^{-8}$ or better — i.e., very much closer to zero, or effectively zero. Keeping in mind the order of magnitude of $\mathscr{R}e(\bar{\omega})$, we conclude that the P-C system with reverse U and hence the C-P system also are conservative. The critical flow velocities for

‡ As reported in Païdoussis (2001), a similar situation arises in the study of fluid-conveying pinned–clamped and clamped–pinned pipes modelled as beams. Calculations with not so accurate λ's yielded $\mathscr{I}m(\omega) \neq 0$ for arbitrarily small U, thereby suggesting that the system may be nonconservative! Significantly, correctness to 4 significant figures is quite sufficient for the pinned–clamped system to obtain $\mathscr{I}m(\omega) = 0$, but even 8 significant-figure accuracy is not good enough for the clamped–pinned one.

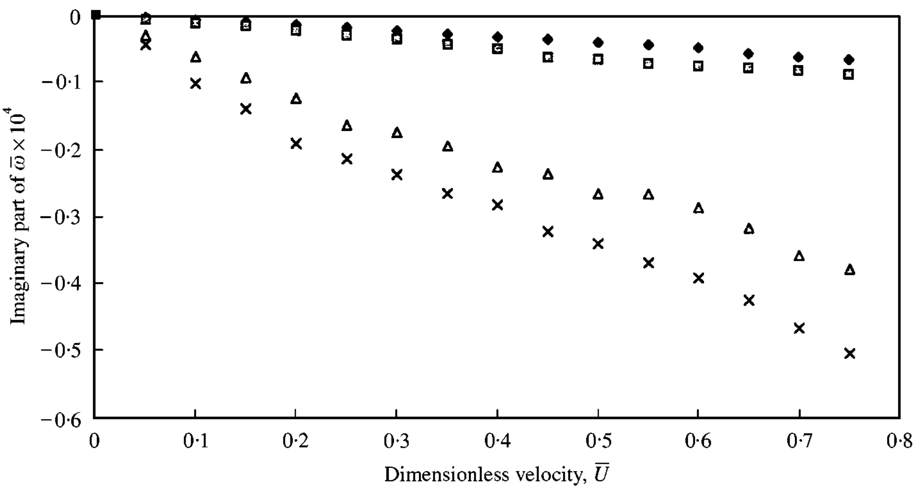

Figure 7. The effect of tolerance in the calculation of the imaginary component of $\bar{\omega}$ versus $\bar{U}$ for the rubber–air system, analysed by the travelling-wave method, for $n = m = 2$: $\times$, double precision; $\triangle$, long double precision; $\square$, tolerance of 10^{-6}; ◆, tolerance of 10^{-8}.

divergence and for subsequent coupled-mode flutter are the same for both clamped-pinned and pinned-clamped systems.

Finally, it should be recalled that, in all the foregoing, structural damping was taken to be zero. If even a small amount of dissipation is taken into account, however, the asymmetric boundary condition "flow-induced damping" disappears (in the sense of being overwhelmed) since it is so small. In one case, for a clamped–pinned shell, Wong (2000) shows that the inclusion of mechanical damping as small as 0·12% of the critical is sufficient to nullify the effect of the numerically found flow-induced negative damping.

5. ENERGY CONSIDERATIONS

The fluid forces acting on the system may be described by the perturbation pressure, equation (14) in the context of the travelling-wave solution, which may be rewritten (Païdoussis 1987) as

$$p = -\rho a I(n, \lambda) \left(\frac{\partial}{\partial t} + U \frac{\partial}{\partial x} \right)^2 w, \tag{22}$$

where $I(n, \lambda)$ is the functional of the Bessel functions in equation (14). Hence, the rate of work done by the fluid on the shell in the course of oscillatory motions is

$$\frac{\mathrm{d}W}{\mathrm{d}t} = -\int_0^L \int_0^{2\pi} \frac{\partial w}{\partial t} \left\{ \rho a I(n, \lambda) \left[\left(\frac{\partial}{\partial t} + U \frac{\partial}{\partial x} \right)^2 w \right] \right\} a \, \mathrm{d}\theta \, \mathrm{d}x. \tag{23}$$

For convenience, we can write $w(x, \theta, t) = \bar{w}(x, t) \cos n\theta$. Hence, for harmonic oscillations, the work done over a period of oscillation, T, is

$$\Delta W = -\rho \pi a^2 \int_0^T \int_0^L \frac{\partial \bar{w}}{\partial t} \left\{ I(n, \lambda) \left[\left(\frac{\partial}{\partial t} + U \frac{\partial}{\partial x} \right)^2 \bar{w} \right] \right\} \mathrm{d}x \, \mathrm{d}t.$$

Then, integrating by parts (Païdoussis 1998, Section 3.2), this gives

$$\Delta W = -\rho\pi a^2 U I(n,\lambda)\int_0^T \left[\left(\frac{\partial \bar{w}}{\partial t}\right)^2 + U\left(\frac{\partial \bar{w}}{\partial x}\right)\left(\frac{\partial \bar{w}}{\partial t}\right)\right]_0^L \mathrm{d}t. \tag{24}$$

It is, therefore, clear that for supported ends, such that radial displacement and hence $(\partial\bar{w}/\partial t) = 0$ at $x = 0$ and L, one obtains $\Delta W = 0$ and reaches the conclusion that the system is conservative.

This may be thought to clinch the argument. Not necessarily and unequivocally so, however, similarly to the question of existence of coupled-mode flutter of pipes with supported ends (Païdoussis 1998, Section 3.4). For that problem, energy arguments such as the above suggest that flutter is impossible, since $\Delta W = 0$, whereas eigenfrequency calculations show it to be quite possible (and with large $\mathscr{I}m(\omega)$).† Happily, in the case of the shells considered here, both approaches point to the same conclusion.

6. CONCLUSIONS

The dynamics and stability of pinned–clamped and clamped–pinned shells subjected to internal flow were considered. Two methods were used for the analysis: the travelling-wave method and the Fourier-transform approach. To start with, the two methods were applied to clamped–clamped systems, and the results obtained were compared to the existing ones. The agreement was quite good. Next, the clamped–pinned and pinned–clamped systems were considered. Both methods suggested that the clamped–pinned systems are subjected to negative damping for any arbitrarily small flow velocity greater than zero. The pinned–clamped systems, on the other hand, are subjected to positive damping.

In order to ascertain the validity of these results, a careful analysis of sources of numerical errors was carried out. Furthermore, all subsequent calculations were carried out in quadruple precision. The major contribution to inaccuracy of the results from the Fourier-transform method comes from the inaccuracies in the beam eigenvalues. The calculations were repeated for the clamped–pinned rubber–air system by varying systematically the number of accurate significant digits in the beam eigenvalues. It was noted that the magnitude of the negative damping decreased rapidly and monotonically with an increase in the number of accurate significant digits. This indicates that, in the limit, the damping will approach zero.

The most important source of error in the travelling-wave method is the inaccuracy in the determination of λ's appearing in equation (12). Calculations were repeated with the values of λ's obtained with various tolerances. It was noticed that, when tighter tolerances are used to determine the λ's, the magnitude of the negative damping of the clamped–pinned system reduces monotonically. Again, in the limit, the damping should become zero.

The interesting thing about this numerical artefact is that, in some cases at least, it mimics true, physical dynamical behaviour, as seen in Figures 4 and 7 for the rubber–air system. Thus, unlike typical numerical problems when a steady or random oscillatory deviation from the true value (in this case $\mathscr{I}m(\bar{\omega}) = 0$) occurs, what is obtained here is a more or less linear variation of $\mathscr{I}m(\bar{\omega})$ with $\bar{U}$, which seems physically plausible.

Finally, by means of energy considerations, the work done by the fluid on the shell in the course of periodic oscillations is found to be naught. Hence, no energy transfer from the fluid to the shell, or *vice versa*, can occur—at least in the context of linear dynamics.

† In that case, the question was settled by nonlinear theory (Holmes 1978).

It is concluded that both clamped–pinned and pinned–clamped systems are conservative; the small negative damping of the former system and the positive damping of the latter in the numerical results, for any arbitrarily small flow velocity, are simply numerical artefacts.

ACKNOWLEDGEMENTS

The authors gratefully acknowledge the support given to this research by the Natural Sciences and Engineering Research Council of Canada and the programme FCAR of Québec.

REFERENCES

HOLMES, P. J. 1978 Pipes supported at both ends cannot flutter. *Journal of Applied Mechanics* **45,** 619–622.

HORÁČEK, J. & ZOLOTAREV, I. 1984 Influence of fixing the edges of a cylindrical shell with conveying fluid on its dynamic characteristics. *Soviet Applied Mechanics* **20,** 756–765.

MATSUZAKI, Y. & FUNG, Y. C. 1977 Unsteady fluid dynamic forces on a simply-supported circular cylinder of finite length conveying a flow, with application to stability analysis. *Journal of Sound and Vibration* **54,** 317–330.

PAÏDOUSSIS, M. P. 1987 Flow-induced instabilities of cylindrical structures. *Applied Mechanics Reviews* **40,** 163–175.

PAÏDOUSSIS, M. P. 1998 *Fluid-Structure Interactions: Slender Structures and Axial Flow*, Vol. 1. London: Academic Press.

PAÏDOUSSIS, M. P. 2001 *Fluid–Structure Interactions: Slender Structures and Axial Flow*, Vol. 2. London: Academic Press.

PAÏDOUSSIS, M. P. & DENISE, J. P. 1971 Flutter of cylindrical shells conveying fluid. *Journal of Sound and Vibration* **16,** 459–461.

PAÏDOUSSIS, M. P. & DENISE, J. P. 1972 Flutter of thin cylindrical shells conveying fluid. *Journal of Sound and Vibration* **20,** 9–26.

PAÏDOUSSIS, M. P., CHAN, S. P. & MISRA, A. K. 1984 Dynamics and stability of coaxial cylindrical shells containing flowing fluid. *Journal of Sound and Vibration* **97,** 201–235.

PAÏDOUSSIS, M. P., TIAN, B. & MISRA, A. K. 1993 The dynamics and stability of pinned-clamped coaxial cylindrical shells conveying viscous flow. *Proceedings of the Canadian Congress of Applied Mechanics*, *CANCAM 93*, Queen's University, Kingston, Ontario, pp. 259–260.

SHAYO, L. K. & ELLEN, C. H. 1974 The stability of finite length circular cross-section pipes conveying inviscid fluid. *Journal of Sound and Vibration* **37,** 535–545.

WEAVER, D. A. & MYKLATUN, B. 1973 On the stability of thin pipes with an internal flow. *Journal of Sound and Vibration* **31,** 399–410.

WEAVER, D. S. & UNNY, T. E. 1973 On the dynamic stability of fluid-conveying pipes. *Journal of Applied Mechanics* **40,** 48–52.

WONG, S. S. T. 2000 The dynamics of shells conveying fluid, with pinned–clamped and clamped–pinned boundary conditions. M.Eng. thesis, Department of Mechanical Engineering, McGill University, Montreal, QC, Canada.

ZOLOTAREV, I. 1987 Optimization of aerodynamic damping of a cylindrical shell with flowing fluid with the aid of boundary conditions. *Mashinovedenie* **1,** 49–55.